Motion of a vortex line near the boundary of a semi-infinite uniform condensate

Peter Mason,[1] Natalia G. Berloff,[1] and Alexander L. Fetter[2]
[1]*Department of Applied Mathematics and Theoretical Physics, University of Cambridge, Wilberforce Road, Cambridge, CB3 0WA, United Kingdom*
[2]*Departments of Physics and Applied Physics, Stanford University, Stanford, California 94305-4045, USA*
(Received 26 May 2006; published 18 October 2006)

We consider the motion of a vortex in an asymptotically homogeneous condensate bounded by a solid wall where the wave function of the condensate vanishes. For a vortex parallel to the wall, the motion is essentially equivalent to that generated by an image vortex, but the depleted surface layer induces an effective shift in the position of the image compared to the case of a vortex pair in an otherwise uniform flow. Specifically, the velocity of the vortex can be approximated by $U \approx (\hbar/2m)(y_0 - \sqrt{2}\xi)^{-1}$, where y_0 is the distance from the center of the vortex to the wall, ξ is the healing length of the condensate, and m is the mass of the boson.

DOI: 10.1103/PhysRevA.74.043611 PACS number(s): 03.75.Lm, 05.45.−a, 67.40.Vs, 67.57.De

I. INTRODUCTION

Vortex dynamics in a Bose-Einstein condensate (BEC) has been studied intensively, initially in the context of superfluid helium and later in dilute trapped BECs. The motion of vortices in both uniform and inhomogeneous condensates has been the subject of many theoretical works, and extensive reviews of these efforts have been given in [1,2].

In this paper we consider the problem of vortex motion in an asymptotically homogeneous condensate in the presence of a solid wall where the wave function of the condensate vanishes. Recent discussions (see, for example, [3,4] and references therein) on the motion of vortices near the surface of trapped condensates have questioned the relevance of the method of images in describing this motion. In that case, the nonuniform condensate density is approximated by a linear function that vanishes at the Thomas-Fermi surface. The resulting vortex motion can be considered to arise principally from the local density gradient caused by the trapping potential.

Here, we consider a rather different situation, in which the condensate density approaches its bulk value within a healing length ξ, and the vortex is located in the asymptotically uniform region. In this latter case, the local gradient of the condensate density is very small. The motion can be interpreted as arising from an image, but the depleted surface layer induces an effective shift in the position of the image in comparison with the case of a uniform incompressible fluid.

Our geometry is two-dimensional, with the vortex aligned along the z axis, parallel to the surface of the wall. The dynamics of the time-dependent BEC in the presence of the solid wall at $y=0$ is described by the Gross-Pitaevskii (GP) equation

$$-2i\psi_t = \nabla^2\psi + (1-|\psi|^2)\psi, \tag{1}$$

subject to the boundary conditions

$$\psi(x, y=0, t) = 0, \quad 0 \leqslant y < \infty, \quad |x| < \infty, \tag{2}$$

in dimensionless units, such that the distance is measured in healing lengths $\xi = \hbar/\sqrt{2mgn_0}$, where g is a two-dimensional coupling constant with dimension of energy times area, m is the mass of the boson, and n_0 is the bulk number density per unit area. Time is measured in units of $m\xi^2/\hbar$ and energy in units of $\hbar^2 n_0/m$. In our units, the speed of sound c in the bulk condensate is $c = 1/\sqrt{2}$.

In the absence of vortices, the exact solution of Eq. (1) for the stationary state of the semi-infinite condensate is

$$f(y) = \tanh(y/\sqrt{2}). \tag{3}$$

In classical inviscid fluid dynamics with constant mass density ρ, the relevant kinematic boundary condition at a solid wall with normal vector $\mathbf{n}$ is

$$\rho \mathbf{u} \cdot \mathbf{n} = 0, \tag{4}$$

where ρ is the local density of the fluid and $\mathbf{u}$ is the velocity of the fluid. The corresponding problem of a vortex moving parallel to the wall is solved by placing one or more image vortices in such a way that condition (4) is identically satisfied.

For the dynamics described by the GP equation (1), the density $\rho \propto |\psi|^2$ is no longer constant, but rather vanishes at the surface of the wall. Thus condition (4) is automatically satisfied, and all components of $\mathbf{u}$ can in principle remain finite on the boundary. Therefore it may seem that image vortices are irrelevant in the case of the GP equation, so that the vortex should remain stationary away from the boundary (where the fluid density is constant apart from exponentially small corrections). Our numerical simulations show that this is not true. In fact, the vortex moves parallel to the boundary, and it moves *faster* than a corresponding pair of vortices of opposite circulation in a uniform condensate in the absence of the depletion caused by the boundary. The purpose of our paper is to study this motion in detail.

The paper is organized as follows. In Sec. II we find the family of disturbances moving with a constant velocity along the solid wall by numerically solving the Gross-Pitaevskii (GP) equation in the frame of reference moving with the disturbance. In Sec. III a time-dependent Lagrangian variational analysis is used to find the first two leading terms in the equation of the vortex motion in the limit of large distance from the wall. In Sec. IV an alternative approach based on the dependence of total energy and momentum on the vortex position is used to determine the vortex velocity. In

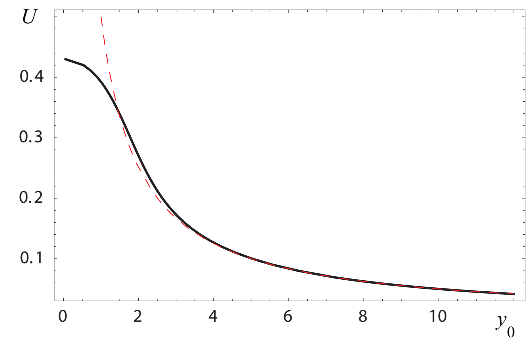

FIG. 1. (Color online) Graphs of the velocity of the vortex U vs the vortex position y_0 as calculated via numerical integration of Eq. (5) subject to the boundary conditions $\psi \to 1$ as $x^2+y^2 \to \infty$ without the wall (solid line) and the asymptotics given by $U=(2y_0)^{-1}$ (dashed line). All quantities are dimensionless, with the healing length ξ as a unit of length and $\hbar/m\xi$ as a unit of velocity.

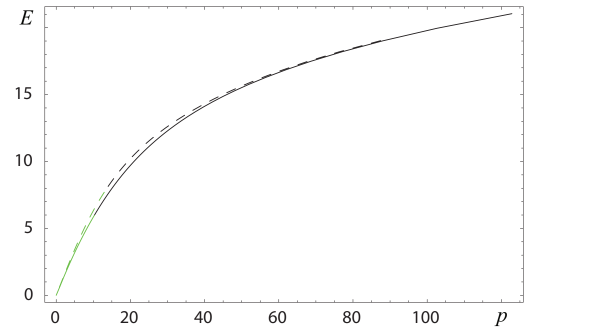

FIG. 2. (Color online) The momentum-energy curve of the solitary wave solutions of Eq. (5) with the solid wall (solid line) and the JR dispersion curve (dashed line) that has no solid wall. For the solid-wall boundary condition, the vortex solutions with nonzero vorticity and nodes are shown in black and the vorticity-free solutions in gray (green). All quantities are dimensionless, with $\hbar^2 n_0/m$ as unit of energy and $\hbar/\xi$ as unit of momentum.

Sec. V we summarize our main findings and compare with the vortex motion in other related geometries.

II. NUMERICAL SOLUTIONS

In what follows we seek solitary-wave solutions of Eq. (1) that preserve their form as they move parallel to the wall with fixed velocity U. For each value of the velocity U, we have

$$\psi(x,y,t) = \psi(\eta,y),$$

where $\eta = x - Ut$. The GP equation (1) becomes

$$2iU\psi_x = \nabla^2\psi + (1-|\psi|^2)\psi, \tag{5}$$

where we set $x=\eta$. In the absence of the wall, the solitary-wave solutions of Eq. (5) were found by Jones and Roberts [5]. For each value of U, there is a well-defined momentum p and energy E, given by

$$p = \frac{1}{2i}\int [(\psi^* - 1)\partial_x\psi - (\psi - 1)\partial_x\psi^*]dxdy, \tag{6}$$

$$E = \frac{1}{2}\int |\nabla\psi|^2 dxdy + \frac{1}{4}\int (1-|\psi|^2)^2 dxdy. \tag{7}$$

In a momentum-energy pE plot, the family of such solitary-wave solutions consists of a single branch that terminates at $p=0$ and $E=0$ as $U\to c$ (we call this curve the "JR dispersion curve"). For small U and large p and E, the solutions are asymptotic to pairs of vortices of opposite circulation. As p and E decrease from infinity, the solutions begin to lose their similarity to vortex pairs. Eventually, for a velocity $U\approx 0.43$ (momentum $p_0\approx 7.7$ and energy $E_0 \approx 13.0$) they lose their vorticity (ψ loses its zero), and thereafter the solutions may better be described as "rarefaction waves" that can be thought of as finite amplitude sound waves. The velocity of the vortex pair in the absence of the boundary is plotted as a function of the position of the vortices $\pm y_0$ shown in Fig. 1. The dashed line gives the asymptotic velocity valid for large y_0 as $U=(2y_0)^{-1}$.

In analogy with these results, we used numerical methods to find the complete family of solitary-wave solutions of Eq. (5) subject to the hard-wall boundary condition (2). Specifically, we mapped the semi-infinite domain onto the box $(-\frac{\pi}{2},\frac{\pi}{2})\times(0,\frac{\pi}{2})$ using the transformation $\hat{x}=\tan^{-1}(Dx)$ and $\hat{y}=\tan^{-1}(Dy)$, where $D\sim 0.4-1.5$. The transformed equations were expressed in a second-order finite-difference form using 200^2 grid points, and the resulting nonlinear equations were solved by the Newton-Raphson iteration procedure, using a banded matrix linear solver based on the biconjugate gradient stabilized iterative method with preconditioning. Similar to [5], we are interested in finding the dispersion curve for our solutions in the pE plane. The energy and impulse of each solitary wave are defined by the expressions (6) and (7) appropriately modified for the "ground state" given by $f(y)$:

$$p = \frac{1}{2i}\int \{[\psi^* - f(y)]\partial_x\psi - [\psi - f(y)]\partial_x\psi^*\}dxdy, \tag{8}$$

$$E = \frac{1}{2}\int \left[|\nabla\psi|^2 + \frac{1}{2}(1-|\psi|^2)^2 - \mathrm{sech}^4(y/\sqrt{2})\right]dxdy. \tag{9}$$

In Fig. 2, we show the resulting solutions in the pE plane. The plot of the velocity dependence on the vortex position is given below in Fig. 3 in Sec. IV. All our vortex solutions with a rigid wall (those with a node in the fluid's interior) move with velocities less than $U=0.47$. For $U>0.47$, the zero of the wave function occurs on the wall only, and the solitary waves resemble rarefaction pulses of the JR dispersion curve away from the wall.

III. VARIATIONAL APPROACH

The time-dependent variational Lagrangian method offers a convenient analytical approach to estimate the vortex velocity for large y_0. The dimensionless GP equation is the Euler-Lagrange equation for the time-dependent Lagrangian functional

$$\mathcal{L} = \mathcal{T} - \mathcal{E} \equiv \frac{1}{2} i \int (\psi^* \psi_t - \psi_t^* \psi) dxdy - \frac{1}{2} \int \left(|\nabla \psi|^2 + \frac{1}{2} |\psi|^4 \right) dxdy, \tag{10}$$

where the time-dependent terms constitute the "kinetic energy" $\mathcal{T}$ and the remaining terms are the GP energy functional $\mathcal{E}$.

We assume a trial function that depends on one or more parameters, and use this trial function to evaluate the Lagrangian $\mathcal{L}$ in Eq. (10), which will depend on the parameters and their first time derivatives. The resulting Euler-Lagrange equations determine the dynamical evolution of the parameters. For the present problem of a vortex moving parallel to a rigid boundary with the boundary condition (2), the vortex coordinates (x_0, y_0) serve as the appropriate parameters, where $-\infty < x_0 < \infty$ and $0 < y_0 < \infty$.

When the condensate contains a vortex at a distance y_0 from the boundary, the original condensate wave function (3) acquires both a phase $S(\mathbf{r}, \mathbf{r}_0)$ and a modulation near the center of the vortex, where the density vanishes. To model this behavior for the half space, it is preferable to include an image vortex at the image position $(x_0, -y_0)$. In this case, the approximate variational contribution to the phase is

$$S(\mathbf{r}, \mathbf{r}_0) = \arctan\left(\frac{y - y_0}{x - x_0} \right) - \arctan\left(\frac{y + y_0}{x - x_0} \right). \tag{11}$$

Here, the image vortex cuts off the long-range tail of the velocity, giving a convergent kinetic energy even for a semi-infinite condensate. It thus seems more physical to include the image in this particular geometry, even though the image is often omitted for the highly nonuniform density obtained in the Thomas-Fermi limit for a trapped condensate [3,4,6,7].

In addition, the vortex affects the density near its core, which is modeled by a factor $a(|\mathbf{r} - \mathbf{r}_0|)$, where $a(r)$ vanishes linearly for small $r = \sqrt{x^2 + y^2}$ and $a(r) \to 1$ for $r \gg 1$ [4]. In principle, the function $a(r)$ can be taken as the exact radial solution of the Gross-Pitaevskii equation in an unbounded condensate, but this choice requires numerical analysis, and it is often preferable to use a variational approximation. A particularly simple choice is [8]

$$a(r) = \begin{cases} r/\lambda & \text{for } r \leqslant \lambda, \\ 1 & \text{for } r \geqslant \lambda, \end{cases} \tag{12}$$

where λ is the effective vortex core size; a variational analysis yields the optimal value $\lambda = \sqrt{6}$. With these various approximations, the variational trial function is [4]

$$\psi(\mathbf{r}, \mathbf{r}_0, t) = e^{iS(\mathbf{r}, \mathbf{r}_0)} f(y) a(|\mathbf{r} - \mathbf{r}_0|). \tag{13}$$

The time-dependent part of the functional in Eq. (10) becomes

$$\mathcal{T} = -\int [f(y)]^2 \partial_t S |a(|\mathbf{r} - \mathbf{r}_0|)|^2 dxdy \approx -\int [f(y)]^2 \partial_t S dxdy, \tag{14}$$

where the last approximation omits the effect of the vortex on the density, replacing $|a|^2$ by 1 throughout the condensate. A straightforward analysis then yields

$$\mathcal{T} \approx 2\pi \dot{x}_0 \int_0^{y_0} [f(y)]^2 dy, \tag{15}$$

where $\dot{x}_0$ is the velocity U of the vortex parallel to the wall. The contribution to $\mathcal{T}$ from the vortex core yields a term that is smaller than Eq. (15) by a factor of relative order y_0^{-2}, which is negligible relative to the leading correction of order y_0^{-1} that we retain here.

Since the energy functional will turn out to depend only on the single coordinate y_0, the Euler-Lagrange equation for x_0 implies that y_0 remains constant (as expected from energy considerations). In contrast, the equation for y_0 reduces to

$$\frac{d}{dt} \frac{\partial \mathcal{L}}{\partial \dot{y}_0} = \frac{\partial \mathcal{L}}{\partial y_0} = 0, \tag{16}$$

since $\dot{y}_0$ does not appear in $\mathcal{T}$ (and hence in $\mathcal{L}$). Thus the dynamical motion of the vortex is given by

$$\dot{x}_0 \approx \frac{1}{2\pi [f(y_0)]^2} \frac{\partial \mathcal{E}}{\partial y_0}. \tag{17}$$

It is evident that only the derivative $\partial \mathcal{E} / \partial y_0$ is relevant. Several terms in $\mathcal{E}$ are constant for large y_0 and thus play no role in the present analysis. The dominant contribution is the kinetic energy $\mathcal{E}_{kv} = \frac{1}{2} \int |\nabla S|^2 |\psi|^2 dxdy$ arising from the circulating vortex flow. The squared velocity now follows from Eq. (11), and the resulting flow-induced kinetic energy is

$$\mathcal{E}_{kv} = \frac{1}{2} \int f(y)^2 a(|\mathbf{r} - \mathbf{r}_0|)^2 |\nabla S|^2 dxdy. \tag{18}$$

This quantity can be evaluated by first integrating over the variable x and then expanding $\partial \mathcal{E}_{kv} / \partial y_0$ for large y_0. When we neglect terms of order $1/y_0^3$, the translational velocity reduces to

$$U \approx \frac{1}{2y_0} \left(1 + \frac{\sqrt{2}}{y_0} \right), \tag{19}$$

which is independent of λ to this order in $y_0 \gg 1$.

IV. VORTEX VELOCITY THROUGH THE HAMILTONIAN RELATIONSHIP BETWEEN ENERGY AND IMPULSE

In this section we present a different approach to the asymptotics for the vortex velocity based on the relationship between energy and momentum of the vortex pair. We compare the motion of a pair of vortices of opposite circulation (JR solutions) that satisfy

$$2iU_1 \psi_{1x} = \nabla^2 \psi_1 + (1 - |\psi_1|^2) \psi_1, \quad |\psi_1| \to 1, \quad |\mathbf{x}| \to \infty, \tag{20}$$

with the motion of a vortex next to the solid wall

$$2iU_2\psi_{2x} = \nabla^2\psi_2 + (1-|\psi_2|^2)\psi_2, \quad |\psi_2| \to |\tanh(y/\sqrt{2})|, \tag{21}$$

$$|\mathbf{x}| \to \infty.$$

For the asymptotics, we are interested in the solutions for small U_i, for $i=1,2$, that correspond to a pair of vortices of opposite circulation. We calculate the following quantities: the position of the pair $(0,\pm y_0)$, the energy and impulse given by Eqs. (7) and (6) for $i=1$ and by (9) and (8) for $i=2$, so that

$$U_i = \frac{\partial E_i}{\partial p_i}. \tag{22}$$

These expressions for $i=1$ were derived in [5,9]; similar arguments immediately lead to the expressions for $i=2$.

Note that U_i, E_i, and p_i are functions of y_0 and if $y_0 \gg 1$,

$$E_1 = 2\pi\log(2y_0), \quad p_1 = 4\pi y_0, \tag{23}$$

(see, for instance, [10]). From Eq. (22) we have

$$U_1 = \frac{\partial E_1/\partial y_0}{\partial p_1/\partial y_0} = \frac{1}{2y_0}, \tag{24}$$

as expected.

For large y_0 an accurate approximation to the solution of Eq. (20) for the uniform flow was found [11] as $\psi_1 = u_1(x,y) + iv_1(x,y)$ where

$$u_1(x,y) = (x^2+y^2-y_0^2)\tilde{R}[\sqrt{x^2+(y-y_0)^2}]\tilde{R}[\sqrt{x^2+(y+y_0)^2}],$$

$$v_1(x,y) = -2xy_0\tilde{R}[\sqrt{x^2+(y-y_0)^2}]\tilde{R}[\sqrt{x^2+(y+y_0)^2}], \tag{25}$$

where $\tilde{R}(r) = \sqrt{(0.3437+0.0286r^2)/(1+0.3333r^2+0.0286r^4)}$. Another accurate choice is $\tilde{R}(r) = (r^2+2)^{-1/2}$. Similarly, we expect that ψ_2 is accurately approximated by $\psi_2 = \psi_1|\tanh(y/\sqrt{2})|$.

The question we pose is: What is the position of the vortex $(0,y_0)$ moving parallel to the solid wall with the same velocity as the vortex pair at $(0,y_0-l)$ in the uniform flow? Thus we seek the solution of

$$U_1[y_0 - l(y_0)] = U_2(y_0) = \frac{\partial E_2/\partial y_0}{\partial p_2/\partial y_0}, \tag{26}$$

where we explicitly indicate the dependence of U_1 and U_2 on the vortex position. Since $U_1(y_0-l) = [2(y_0-l)]^{-1}$, we obtain the expression for the shift in the vortex position, l, in the presence of the wall as

$$l(y_0) = y_0 - \frac{1}{2}\frac{\partial p_2/\partial y_0}{\partial E_2/\partial y_0}. \tag{27}$$

We rearrange the right-hand side of Eq. (27) and use Eq. (23) to obtain the final equation that determines $l(y_0)$:

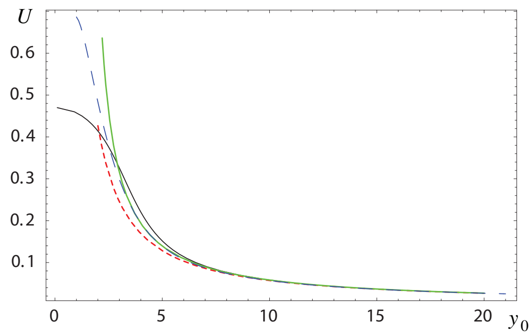

FIG. 3. (Color online) Graphs of the vortex velocity U vs its distance from the wall y_0 as calculated via numerical integration of Eq. (21) (black solid line) and the asymptotics given by Eq. (19) (red short-dashed line) and by Eq. (31) (green solid line). Also shown is the velocity of the vortex calculated by numerically integrating the right-hand side of Eq. (26) (blue long-dashed line). As one can see the simplifications made to derive Eq. (31) are consistent with the full expression (26) for $y_0 > 4$. As in Fig. 1, U and y_0 are both dimensionless.

$$l(y_0) = y_0 - \frac{1}{2}\frac{4\pi + \tilde{dp}}{2\pi/y_0 + \tilde{dE}}, \tag{28}$$

where $\tilde{dE} = \partial(E_2 - E_1)/\partial y_0$ and $\tilde{dp} = \partial(p_2-p_1)/\partial y_0$ in the integral form given by Eqs. (7) and (6) for E_1 and p_1 and Eqs. (9) and (8) for E_2 and p_2. In evaluating the contribution $E_2 - E_1$ only the kinetic terms involving derivatives with respect to x were kept. The integrals $\tilde{dE}$ and $\tilde{dp}$ are exactly integrable in x with the use of MATHEMATICA, in which the leading order terms in $1/y_0$ are given by

$$\tilde{dp} = -\frac{8\pi}{y_0^3}\int_{-\infty}^{\infty}\operatorname{sech}^2(y/\sqrt{2})dy + O(y_0^{-5}),$$

$$\tilde{dE} = \left(\frac{\pi}{y_0^2} + \frac{\pi(\pi^2-18)}{2y_0^4}\right)\int_{-\infty}^{\infty}\operatorname{sech}^2(y/\sqrt{2})dy + O(y_0^{-6}). \tag{29}$$

With $\int_{-\infty}^{\infty}\operatorname{sech}^2(y/\sqrt{2})dy = 2\sqrt{2}$ we finally arrive at

$$l(y_0) = \frac{\sqrt{2}y_0[\pi^2 + 2(y_0^2-5)]}{\sqrt{2}\pi^2 + 2(y_0^3 + \sqrt{2}y_0^2 - 9\sqrt{2})} = \sqrt{2} + O(y_0^{-1}). \tag{30}$$

The vortex next to the wall moves with the velocity

$$U_2 = \frac{1}{2(y_0 - \sqrt{2})}, \tag{31}$$

which is the main result of our asymptotics. Note that if we expand Eq. (31) in a Taylor series we get $U_2 = (2y_0)^{-1}(1 + \sqrt{2}/y_0)$, which agrees with the result (19) of Sec. III. Figure 3 gives the plot of the vortex velocity U as a function of the distance of the vortex from the wall y_0 for the numerical solutions found in Sec. II, asymptotics found in Sec. III [see Eq. (19)], and asymptotics (31).

V. DISCUSSION AND CONCLUSIONS

In a uniform superfluid with a solid boundary, the motion of a quantized vortex arises from the image that enforces the condition of zero normal flow at the wall. This behavior is especially clear for a single vortex at a distance r_0 from the center of a cylindrical container of radius R [6]. For a classical incompressible fluid, the vortex precesses at an angular velocity

$$\dot{\phi}|_{\rm cl} = \frac{\hbar}{m}\frac{1}{R^2 - r_0^2} \qquad (32)$$

because of the image vortex at R^2/r_0.

In a trapped condensate, however, the image is generally omitted [3,4]. Instead, the motion can be considered to arise from the gradient of the trap potential, which produces the gradient in the density in the Thomas-Fermi limit [1]. With the same geometry as for the classical case (32), the precession rate of a vortex in a trapped cylindrical Thomas-Fermi condensate is [1,12–14]

$$\dot{\phi}|_{\rm TF} \approx \frac{\hbar}{m}\frac{\ln(R/\xi)}{R^2 - r_0^2}; \qquad (33)$$

this result is considerably larger than Eq. (32) because of the (typically large) logarithmic factor. Although the denominators of Eqs. (32) and (33) both vary quadratically with r_0, the first result arises from the image and the second from the parabolic trap potential (and thus the parabolic density). If an image is included in the analysis of the trap [15], it adds a correction of order 1 to the large logarithm $\ln(R/\xi)$; such a term is comparable to other terms that are usually omitted.

As an intermediate situation between these two extremes, the present paper has analyzed the dynamics of a vortex in a half space bounded by a solid wall on which the density of condensate vanishes. This geometry represents the simplest problem of a vortex in a condensate interacting with a surface. Since the gradient of the density vanishes exponentially for $y_0 \gg \xi$, only the image remains to drive the motion in the asymptotic region. Our geometry allows us to separate the effect of the surface from the effect of the density gradient, both of which appear in the more complicated problem of an inhomogeneous trapped condensate [3,4]. We found the complete family of solitary-wave solutions moving with subcritical velocities parallel to the wall. In addition, both a variational analysis and the Hamiltonian relationship between energy and momentum were used to give the velocity of the vortex as a function of its distance from the wall. These results are identical through to the first correction term, where the small parameter is the inverse distance from the wall. Our main results are (i) that the vortex moves as if there was an image vortex on the other side of the wall, which essentially replaces the boundary condition (4) with a more stringent requirement $\mathbf{u}\cdot\mathbf{n}=0$ and (ii) that the depleted surface layer induces an effective shift in the position of the image in comparison with the case of the uniform flow. Specifically, the velocity of the vortex can be approximated by

$$U \approx \frac{\hbar}{2m(y_0 - \sqrt{2}\xi)}, \qquad (34)$$

where y_0 is the distance from the center of the vortex to the wall, ξ is the healing length of the condensate, and m is the mass of the boson.

It is important to recognize that Eq. (33) describes the velocity of a vortex in a trapped cylindrical condensate when its position r_0 is relatively far from the condensate boundary ($R-r_0 \gg \xi$). If this condition fails and the vortex is near the boundary, then lengthy analyses using asymptotic (boundary-layer) methods [3] and variational methods [4] yield a rather different result

$$U \approx \frac{\hbar}{2my_0}\ln\left(\frac{y_0}{\delta}\right), \qquad (35)$$

where $y_0=R-r_0$ is the distance from the boundary and δ is a surface thickness (related to the gradient of the density near the boundary).

Although the derivation of Eq. (35) specifically excludes an image vortex, the qualitative form is similar to that for a classical image $U \approx \hbar/2my_0$, apart from the logarithmic factor $\ln(y_0/\delta)$. Analytical approaches used to derive Eq. (33) and other results on the motion of a vortex in a trapped condensate frequently rely on a trial wave function that is formed by the product of the wave function of the individual vortex and the ground state. We anticipate that a trial function should include the image of any vortex that is situated close to the condensate surface. It would be interesting to study how the logarithmic factors in Eqs. (33) and (35) are continuously connected when y_0 becomes comparable with the TF radius R of the trapped condensate; the methods we presented in our paper may well provide the most fruitful approach.

ACKNOWLEDGMENTS

N.G.B. gratefully acknowledges the support from EPSRC (UK). N.G.B. and A.L.F. thank the organizers of the workshop on Ultracold atoms held at the Aspen Center for Physics in June 2005, where this work was started, and Eugene Zaremba for a useful discussion during the workshop. This work was continued at the Warwick workshop on Universal features in turbulence: from quantum to cosmological scales (December 2005); we thank S. Nazarenko and the other organizers for their hospitality.

[1] A. L. Fetter and A. A. Svidzinsky, J. Phys.: Condens. Matter **13**, R135 (2001).
[2] L. M. Pismen, *Vortices in Nonlinear Fields* (Clarendon Press, Oxford, 1999).
[3] J. R. Anglin, Phys. Rev. A **65**, 063611 (2002).
[4] U. Al Khawaja, Phys. Rev. A **71**, 063611 (2005).
[5] C. A. Jones and P. H. Roberts, J. Phys. A **15**, 2599 (1982).
[6] J. K. Kim and A. L. Fetter, Phys. Rev. A **70**, 043624 (2004).
[7] J. K. Kim and A. L. Fetter, Phys. Rev. A **72**, 023619 (2005).
[8] U. R. Fischer and G. Baym, Phys. Rev. Lett. **90**, 140402 (2003).
[9] C. A. Jones, S. J. Putterman, and P. H. Roberts, J. Phys. A **19**, 2991 (1986).
[10] L. P. Pitaevskii and S. Stringari, *Bose-Einstein Condensation* (Clarendon Press, Oxford, 2003), Sec. 5.4.
[11] N. G. Berloff, J. Phys. A **37**, 1617 (2004).
[12] E. Lundh and P. Ao, Phys. Rev. A **61**, 063612 (2000).
[13] D. E. Sheehy and L. Radzihovsky, Phys. Rev. A **70**, 051602(R) (2004).
[14] D. E. Sheehy and L. Radzihovsky, Phys. Rev. A **70**, 063620 (2004).
[15] A. L. Fetter, J. Low Temp. Phys. **113**, 189 (1998).